Convex Optimization for Fast image dehazing

Srujana B - MA17BTECH11001
J Sai Vyshnavi - MA17BTECH11005

04/03/2019

Citation

Jiaxi He ; Cishen Zhang ; Ran Yang ; Kai Zhu , **Convex optimization for fast image dehazing**, 2016 IEEE International Conference on Image Processing (ICIP)

Hazed Vs NonHazed

Introduction

- **Why should we dehaze a image?**
- Image processing has widely used in a number of vision applications such as in self driving cars (images need to be dehazed instantaneously).

Introduction

- **Why is this algorithm better than any other previous algorithm?**
- Since the haze effect reduces the degree of contrast in images, the image dehazing process is to enhance the level of image contrast, which is the general idea of different dehazing algorithms in the literature.
- All the other algorithms use non-convex approach where as CO-HDWT,CO algorithms uses a convex approach.
- Named algorithms include : He,Tarel,Zhung,Meng....

Figure

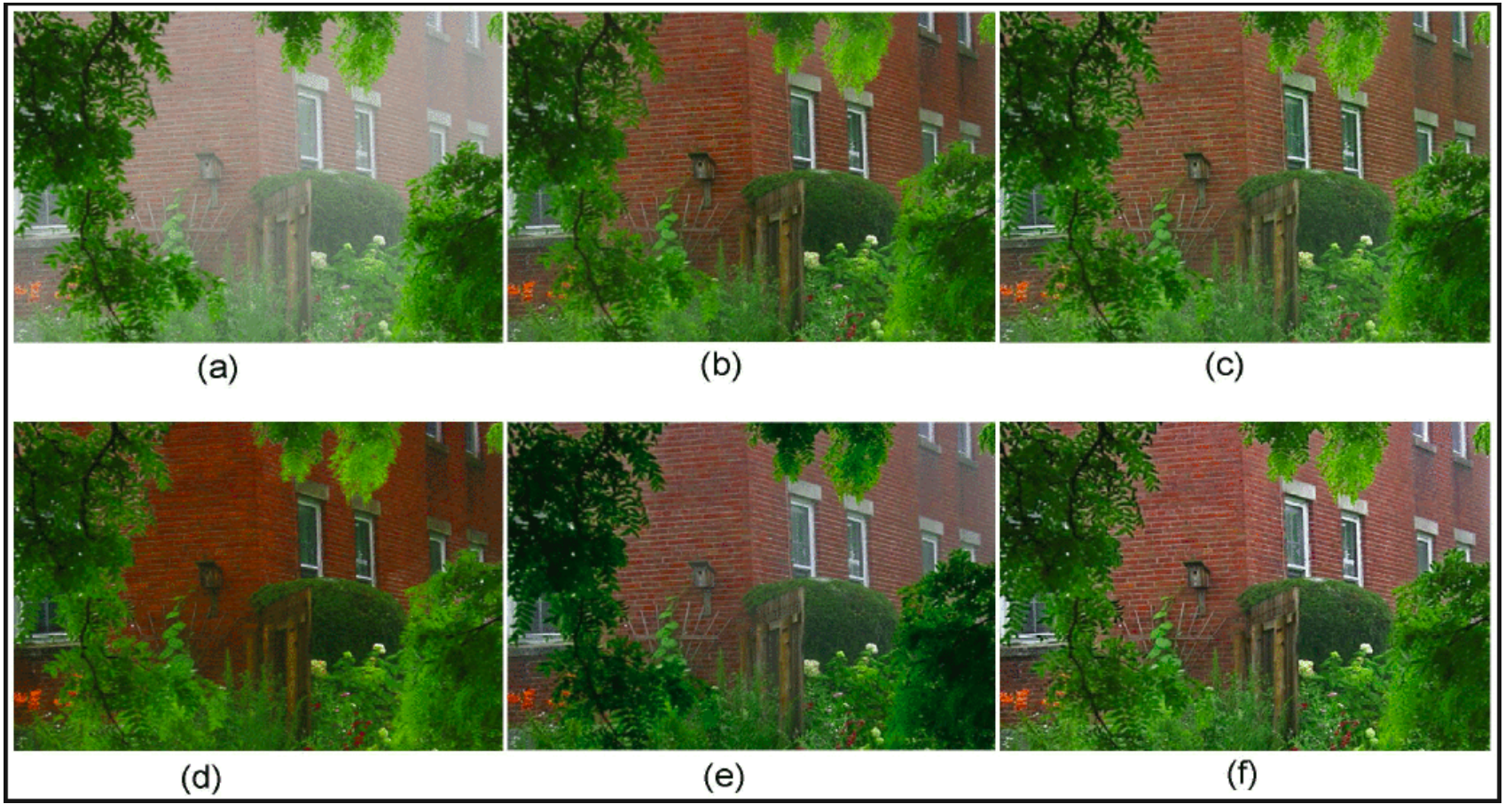

Figure

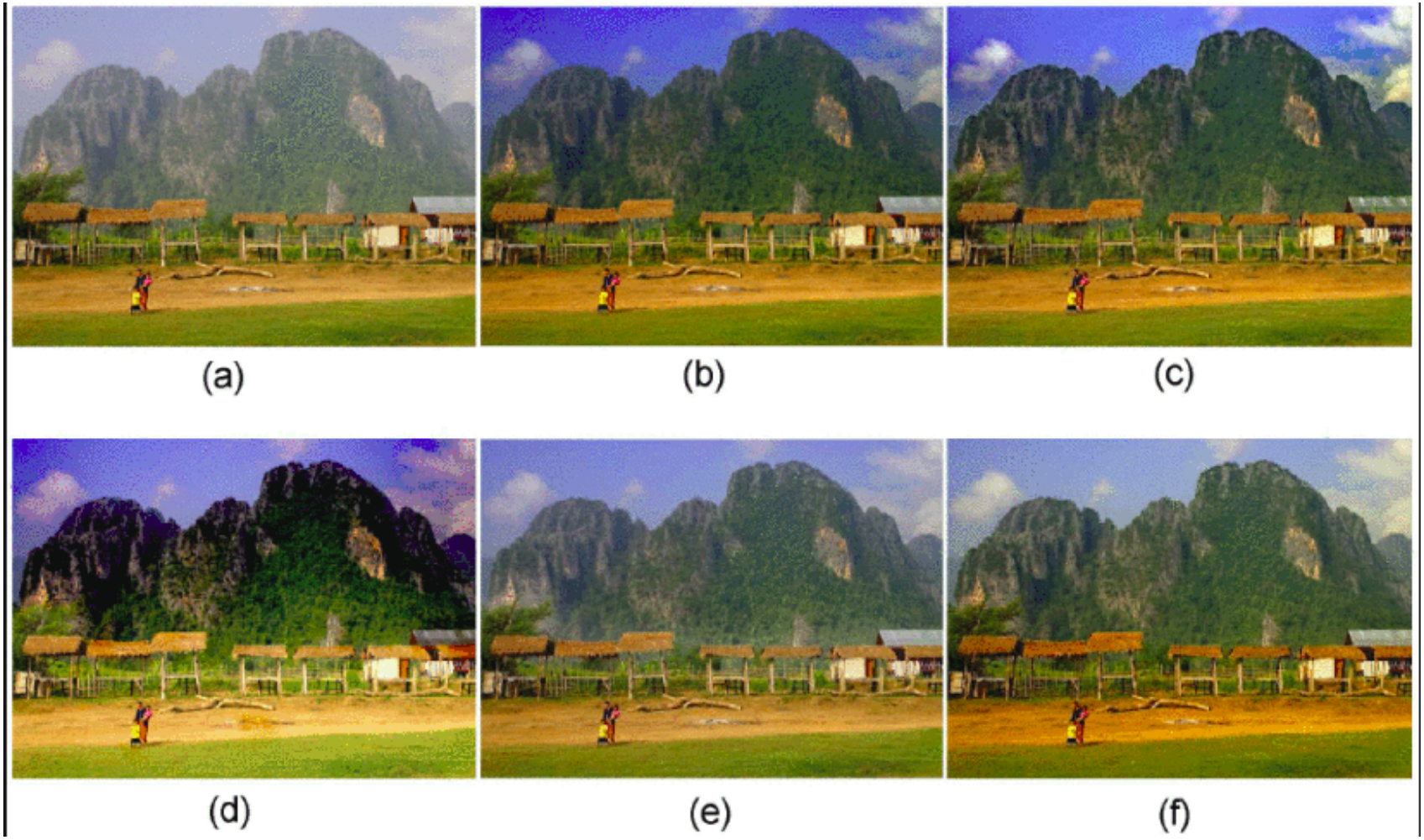

Figure

Comparison of average computational time (second) of different algorithms for images of different sizes

Algorithm \ Size	600×450	1024×768	1536×1024
He et al. [9]	10.04	29.46	65.4
Tarel et al. [21]	8.81	68.90	335.79
Meng et al. [24]	4.782	5.60s	10.27
Zhu et al. [25]	3.68	4.08	8.08
CO	2.25	6.85	12.9
CO-DHWT	0.70	2.08	3.72

Haar Wavelet Transform

In the discrete wavelet transform, every wavelet is implemented through their wavelet filters, low-pass and high-pass. That is, filters of different cut-off frequencies are used to analyse the signal. The signal passes through a series of high-pass filters to analyse its high frequencies, and it passes through a series of low-pass filters to analyse its low frequencies.

The 1-D Discrete Haar Wavelet Transform :

Given two numbers a and b, its DHWT is:

$(a, b) \xrightarrow{DHWT} ((b + a)/2, (b - a)/2)$

The low-pass averaging filter $\tilde{\mathbf{h}}$ and high-pass difference filter $\tilde{\mathbf{g}}$ for DHWT can be respectively represented as:

$$\tilde{\mathbf{h}} = (\frac{1}{2}, \frac{1}{2}), \qquad \tilde{\mathbf{g}} = (-\frac{1}{2}, \frac{1}{2}) \tag{4.2}$$

Then, the so-called 2×2 Haar matrix associated with the DHWT is constructed as:

$$\tilde{\mathbf{W}}_2 = \left[\begin{array}{c} \tilde{\mathbf{h}} \\ \hline \tilde{\mathbf{g}} \end{array}\right] = \begin{bmatrix} \frac{1}{2} & \frac{1}{2} \\ -\frac{1}{2} & \frac{1}{2} \end{bmatrix}. \tag{4.3}$$

where the subscript 2 for $\tilde{\mathbf{W}}$ indicates the dimension of the Haar matrix, in the context $\tilde{\mathbf{W}}_2 \in \mathbb{R}^{2\times 2}$.

Haar Wavelet Transform

Generalisation :

For a signal $\mathbf{v} = [v_1, v_2 \ldots, v_n] \in \mathbb{R}^N$, where $N = 2n$, with n being positive integers, a Haar matrix $\tilde{\mathbf{W}}_N \in \mathbb{R}^{N \times N}$ is built to compute the DHWT of $\mathbf{v}$ as follows:

$$\hat{\mathbf{v}} = \tilde{\mathbf{W}}_N \mathbf{v} = \left[\begin{array}{c} \tilde{\mathbf{H}}_N \\ \hline \tilde{\mathbf{G}}_N \end{array}\right] = \left[\begin{array}{c} \mathbf{E} \otimes \tilde{\mathbf{h}} \\ \hline \mathbf{E} \otimes \tilde{\mathbf{g}} \end{array}\right]$$

$$= \left[\begin{array}{cccccccccc} 1/2 & 1/2 & 0 & 0 & 0 & 0 & \ldots & 0 & 0 \\ 0 & 0 & 1/2 & 1/2 & 0 & 0 & \ldots & 0 & 0 \\ \vdots & & & & \ddots & & & & \vdots \\ 0 & 0 & 0 & 0 & \ldots & 0 & 0 & 1/2 & 1/2 \\ \hline -1/2 & 1/2 & 0 & 0 & 0 & 0 & \ldots & 0 & 0 \\ 0 & 0 & -1/2 & 1/2 & 0 & 0 & \ldots & 0 & 0 \\ \vdots & & & & \ddots & & & & \vdots \\ 0 & 0 & 0 & 0 & \ldots & 0 & 0 & -1/2 & 1/2 \end{array}\right] \cdot \begin{bmatrix} v_1 \\ v_2 \\ v_3 \\ v_4 \\ v_5 \\ \vdots \\ v_{n-1} \\ v_n \end{bmatrix} = \begin{bmatrix} (v_1 + v_2)/2 \\ (v_3 + v_4)/2 \\ \vdots \\ (v_{n-1} + v_n)/2 \\ (v_2 - v_1)/2 \\ (v_4 - v_3)/2 \\ \vdots \\ (v_n - v_{n-1})/2 \end{bmatrix}$$

(4.4)

Haar Wavelet Transform

where $\hat{\mathbf{v}} \in \mathbb{R}^n$ is the DHWT of $\mathbf{v}$, $\mathbf{E}$ is an identity matrix with proper dimensions and $\otimes$ is the Kronecker product.

Accordingly, the inverse process from $\hat{\mathbf{v}}$ to recover $\mathbf{v}$ can also be written as a matrix product:

$$\mathbf{v} = \tilde{\mathbf{W}}_N^{-1}\hat{\mathbf{v}} = \left[\begin{array}{cccc|cccc} 1 & 0 & \dots & 0 & -1 & 0 & \dots & 0 \\ 1 & 0 & & 0 & 1 & 0 & & 0 \\ 0 & 1 & & 0 & 0 & -1 & & 0 \\ 0 & 1 & & 0 & 0 & 1 & & 0 \\ \vdots & & \ddots & \vdots & \vdots & & \ddots & \vdots \\ 0 & 0 & & 1 & 0 & 0 & & -1 \\ 0 & 0 & \dots & 1 & 0 & 0 & \dots & 1 \end{array}\right] \cdot \begin{bmatrix} (v_1+v_2)/2 \\ (v_3+v_4)/2 \\ \vdots \\ (v_{n-1}+v_n)/2 \\ (v_2-v_1)/2 \\ (v_4-v_3)/2 \\ \vdots \\ (v_n-v_{n-1})/2 \end{bmatrix} = \begin{bmatrix} v_1 \\ v_2 \\ v_3 \\ v_4 \\ v_5 \\ v_6 \\ \vdots \\ v_8 \end{bmatrix} \quad (4.5)$$

Haar Wavelet Transform

We know that, an Orthogonal matrix satisfies the following property,

$$U^{-1} = U^T$$

And from (4.4) and (4.5) observe that, $\hat{\mathbf{W}}_N^{-1} = 2\hat{\mathbf{W}}_N^T$

$\implies \hat{\mathbf{W}}_N$ is nearer to a orthogonal matrix.

Haar Wavelet Transform

If we multiply $\tilde{\mathbf{W}}_N$ by $\sqrt{2}$, we then obtain an orthogonal matrix $\mathbf{W}_N$:

$$\mathbf{W_N} = \begin{bmatrix} \mathbf{H}_N \\ \hline \mathbf{G}_N \end{bmatrix} = \begin{bmatrix} \mathbf{E} \otimes \mathbf{h} \\ \hline \mathbf{E} \otimes \mathbf{g} \end{bmatrix} = \left[\begin{array}{ccccccc} \frac{\sqrt{2}}{2} & \frac{\sqrt{2}}{2} & 0 & 0 & \dots & 0 & 0 \\ 0 & 0 & \frac{\sqrt{2}}{2} & \frac{\sqrt{2}}{2} & & 0 & 0 \\ \vdots & & & & \ddots & & \vdots \\ 0 & 0 & 0 & 0 & \dots & \frac{\sqrt{2}}{2} & \frac{\sqrt{2}}{2} \\ \hline -\frac{\sqrt{2}}{2} & \frac{\sqrt{2}}{2} & 0 & 0 & \dots & 0 & 0 \\ 0 & 0 & -\frac{\sqrt{2}}{2} & \frac{\sqrt{2}}{2} & & 0 & 0 \\ \vdots & & & & \ddots & & \vdots \\ 0 & 0 & 0 & 0 & \dots & -\frac{\sqrt{2}}{2} & \frac{\sqrt{2}}{2} \end{array}\right] \tag{4.8}$$

where the orthogonal matrix $\mathbf{W}_N$ is called the DHWT matrix with $\mathbf{W}_N^{-1} = \mathbf{W}_N^T$, and $\mathbf{h} = (\frac{\sqrt{2}}{2}, \frac{\sqrt{2}}{2})$, $\mathbf{g} = (\frac{-\sqrt{2}}{2}, \frac{\sqrt{2}}{2})$ being respectively the low-pass Haar filter and high-pass Haar filter.

Haar Wavelet Transform -2D

Let B $\in R_{+}^{MxN}$ represent the matrix of a grayscale digital image, where M = 2i and N = 2j, with i, j being positive integers.
Step 1: compute the 1-D DHWT of each column of the image by $W_M B$,
with $W_M \in R^{MxM}$ being the DHWT matrix.. In this manner, we obtain a new array with a structure taking the low frequency information in the top half while having the detailed information (i.e. high frequency information) in the bottom half.

Haar Wavelet Transform-2D

(a) Image "Lena", with size 512×512

(b) 1-D DHWT applied to the columns of "Lena"

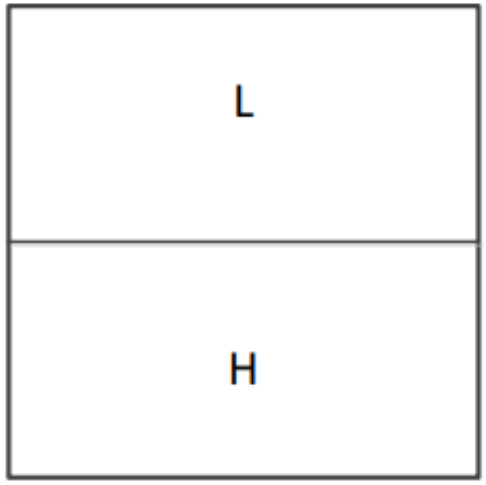

(c) Structure diagram of the image in (b)

(d) 2-D DHWT applied to "Lena"

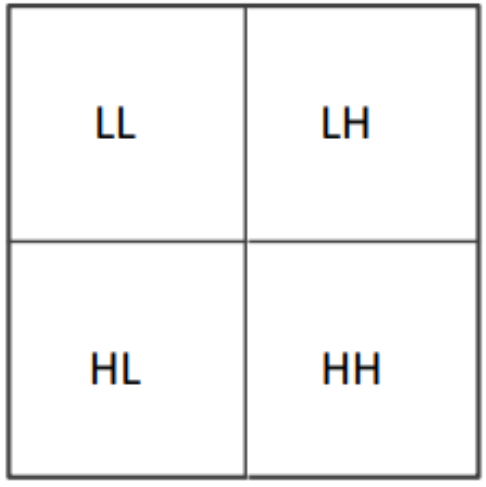

(e) Structure diagram of the image in (d)

Haar Wavelet Transform-2D

Then, the 2-D DHWT of the digital image B is achieved by applying the 1-D DHWT to each row of the already vertically transformed image:

$$\hat{B} = \mathrm{W}_M B W_N^T$$

where, $\hat{B} \in R_+^{MxN}$ is the 2-D DHWT of the image B, and $W_N \in R^{NxN}$ is the DHWT matrix.

Haar Wavelet Transform - 2D

- **LL**: Denoted by (A).
  $\Rightarrow$ Obtained by filtering the original image with **low-pass filter h** along the **columns** and then along **rows** .
  $\Rightarrow$ One fourth the size of the input image, represents the approximated/coarse version of the input image at half the resolution.
- **LH**: Denoted by (H).
  $\Rightarrow$ Derived by filtering **low-pass filter h** $\rightarrow$ columns with followed by **high-pass filter g** $\rightarrow$ rows.
  $\Rightarrow$ Contains the detailed information of the input image in horizontal directions.

Haar Wavelet Transform - 2D

- **HL**: Denoted by (V).
  $\Rightarrow$ Derived by filtering **high-pass filter g** $\rightarrow$ columns with followed by **low-pass filter h** $\rightarrow$ rows
  $\Rightarrow$ The detailed information of the input image in vertical directions can be found in this sub-band image.
- **HH**: Denoted by (D).
  $\Rightarrow$ Derived by filtering **high-pass filter g** $\rightarrow$ columns and rows
  $\Rightarrow$ We can interpret this sub-band image as the area where we find edges of the input image in diagonal direction.

The Hazed Image Model

Let $J_c, I_c \in \mathbb{R}_+^{M \times N}$represent matrices of the haze free and hazed digital RGB color images, respectively, with non negative entries denoted by $J_c(m, n)$ and $I_c(m, n)$ where c=1,2,3 is the color index,$M = 2i, N = 2j$ and m,n $\in \Omega$ are the indices in the 2-dimensional M$\times$N pixel domain Ω.

The Hazed Image Model

The optical model widely used to represent hazed images is:

$$\mathrm{I}_c = \mathrm{J}_c \odot \mathrm{t} + a_c(1 - \mathrm{t}), c = 1, 2, 3, \tag{1}$$

$a_c \rightarrow$ atmospheric light constant of the corresponding color channel
$\mathrm{t} \in \mathbb{R}^{M \times N} \rightarrow$ transmission distribution representing the portion of the light illumination on camera sensors
$\odot \rightarrow$ element wise multiplication operation
$1 \in \mathbb{R}_{+}^{M \times N}$ is the matrix with all 1 as entries.

Model

- In homogeneous atmosphere, t is characterized by $t = e^{-\beta d}$, where d $\in \mathbb{R}^{M \times N}$ is the distance map from the objectives to the camera and β is the scattering coefficient depending on the hazy medium.
  $0 < t <= 1$ (element wise)

Model-Assumptions

- Haze is evenly distributed in atmosphere
- **d** is piecewise constant for most images

$\Longrightarrow$ t is piece wise constant in the sense that

t(2m+i,2n+j) = t(2m,2n)

for m $\in [0, M/2), n \in [0, N/2) and\ i, j = 0, 1.$

Frequency division Haze model

Let W be the well known discrete Haar wavelet transform (DHWT) matrix of appropriate dimension. The single level DHWT of $I_c and J_c, c = 1, 2, 3$, results in their transformed matrices with four $\frac{M}{2} \times \frac{N}{2}$ dimensional subband blocks, i.e.,

$$\hat{\mathbf{I}}_c = \mathbf{W}_M I_c \mathbf{W}_N^T = \begin{bmatrix} \hat{\mathbf{I}}_c^a & \hat{\mathbf{I}}_c^h \\ \hat{\mathbf{I}}_c^v & \hat{\mathbf{I}}_c^d \end{bmatrix}, \hat{\mathbf{J}}_c = W_M J_c \mathbf{W}_N^T = \begin{bmatrix} \hat{\mathbf{J}}_c^a & \hat{\mathbf{J}}_c^h \\ \hat{\mathbf{J}}_c^v & \hat{\mathbf{J}}_c^d \end{bmatrix}.$$

$$W_M = \begin{bmatrix} H^M \\ G^M \end{bmatrix}; W_N = \begin{bmatrix} H^N \\ G^N \end{bmatrix}$$

Model

$$\mathbf{H}^M = \begin{bmatrix} \frac{\sqrt{2}}{2} & \frac{\sqrt{2}}{2} & 0 & 0 & 0 & \cdots & 0 & 0 \\ 0 & 0 & \frac{\sqrt{2}}{2} & \frac{\sqrt{2}}{2} & 0 & \cdots & 0 & 0 \\ & & & & & \ddots & & \\ 0 & 0 & 0 & \cdots & 0 & 0 & \frac{\sqrt{2}}{2} & \frac{\sqrt{2}}{2} \end{bmatrix}_{\frac{M}{2} \times M}$$

and

$$\mathbf{G}^M = \begin{bmatrix} \frac{\sqrt{2}}{2} & -\frac{\sqrt{2}}{2} & 0 & 0 & 0 & \cdots & 0 & 0 \\ 0 & 0 & \frac{\sqrt{2}}{2} & -\frac{\sqrt{2}}{2} & 0 & \cdots & 0 & 0 \\ & & & & & \ddots & & \\ 0 & 0 & 0 & \cdots & 0 & 0 & \frac{\sqrt{2}}{2} & -\frac{\sqrt{2}}{2} \end{bmatrix}_{\frac{M}{2} \times M}$$

Model

It can be verified that, if $\mathbf{t}$ is 2-patch piecewise constant, its DHWT matrix has four identical subband blocks, i.e.,

$$\hat{\mathbf{t}} = \mathbf{W}\mathbf{t}\mathbf{W}^T = \begin{bmatrix} \hat{\mathbf{t}}^a & \hat{\mathbf{t}}^h \\ \hat{\mathbf{t}}^v & \hat{\mathbf{t}}^d \end{bmatrix} = \begin{bmatrix} 2\hat{\mathbf{t}}^1 & 0 \\ 0 & 0 \end{bmatrix}, 0 \prec \hat{\mathbf{t}}^a \preceq 1.$$

where $\hat{\mathbf{t1}}$is the low-pass sub-band distribution of the DHWT of t with its non-negative entries satisfying
$t_1(m, n) = t(2m, 2n), m, n \in \Omega^a$, with Ω^a being the 2-dimensional M/2 x N/2 index set of the low-pass sub-band transmission distribution $\hat{\mathbf{t1}}$.

Model

It can be further verified that the DHWT of the haze model (1) results in

$$\begin{bmatrix} \hat{\mathrm{I}}_c^a & \hat{\mathbf{I}}_c^h \\ \hat{\mathbf{I}}_c^v & \hat{\mathbf{I}}_c^d \end{bmatrix} = \begin{bmatrix} \hat{\mathbf{J}}_c^a \odot \hat{\mathbf{t}}^1 + 2a_c(1-\hat{\mathbf{t}}^1) & \hat{\mathbf{J}}_c^h \odot \hat{\mathbf{t}}^1 \\ \hat{\mathbf{J}}_c^v \odot \hat{\mathbf{t}}^1 & \hat{\mathbf{J}}_c^d \odot \hat{\mathbf{t}}^1 \end{bmatrix}. \tag{2}$$

The low frequency subband block of the above equation presents a DHWT hazed model, with the reduced dimension M/2×N/2, as follows

$$\hat{\mathbf{I}}_c^a = \hat{\mathbf{J}}_c^a \odot \hat{\mathbf{t}}^1 + \ \hat{a}_c(1-\hat{\mathbf{t}}^1),\ \hat{a}_c = 2a_c,\ c = 1,2,3. \tag{3}$$

Proof

Proof: Application of the single-level DHWT to the optical model of a hazed image $\mathbf{I}_c$ leads to:

$$\hat{\mathbf{I}}_c = \mathbf{W}^M \times \mathbf{I}_c \times (\mathbf{W}^N)^T = \begin{bmatrix} \mathbf{H}^M \\ \mathbf{G}^M \end{bmatrix} \times [\mathbf{J}_c \odot \mathbf{t} + a_c(\mathbf{1} - \mathbf{t})] \times \begin{bmatrix} (\mathbf{H}^N)^T & (\mathbf{G}^N)^T \end{bmatrix} \quad (4.20)$$

Proof

Considering the Haar wavelet basis matrix $\mathbf{H}^M$ and $\mathbf{G}^M$ as well as the assumption that $\mathbf{t}$ is 2-patch piecewise constant, it can be easily obtained that:

$$\begin{bmatrix} \mathbf{H}^M \\ \mathbf{G}^M \end{bmatrix} \times a_c \cdot (\mathbf{1} - \mathbf{t}) \times \begin{bmatrix} (\mathbf{H}^N)^T & (\mathbf{G}^N)^T \end{bmatrix} = a_c \cdot \begin{bmatrix} 2 \cdot (\mathbf{1}_{\frac{M}{2} \times \frac{N}{2}} - \hat{\mathbf{t}}_1) & \mathbf{0}_{\frac{M}{2} \times \frac{N}{2}} \\ \mathbf{0}_{\frac{M}{2} \times \frac{N}{2}} & \mathbf{0}_{\frac{M}{2} \times \frac{N}{2}} \end{bmatrix} \tag{4.21}$$

On the other hand, the assumption that $\mathbf{t}$ is 2-patch piecewise constant can also lead to

$$\mathbf{H}^M (\mathbf{J}_c \odot \mathbf{t})(\mathbf{H}^N)^T(m,n) = \left(\frac{1}{4} \sum_{p,q \in \{0,1\}} \mathbf{J}_c(2m-p, 2n-q) \right) \cdot \mathbf{t}(2m, 2n) \tag{4.22}$$

Note the fact that after DHWT, $\hat{\mathbf{J}}_c^a$ is the blur or low-frequency component of image $\mathbf{J}_c$, i.e.

$$\hat{\mathbf{J}}_c^a(m,n) := \mathbf{H}_1^M \mathbf{J}_c (\mathbf{H}_1^N)^T(m,n) = \frac{1}{4} \sum_{p,q \in \{0,1\}} \mathbf{J}_c(2m-p, 2n-q). \tag{4.23}$$

Proof

Therefore, by comparing the above two Equations (4.22) and (4.23), we have:

$$\mathbf{H}^M(\mathbf{J}_c \odot \mathbf{t})(\mathbf{H}^N)^T(m,n) = \hat{\mathbf{J}}_c^a(m,n) \odot \hat{\mathbf{t}}_1(m,n)$$

i.e.

$$\mathbf{H}^M(\mathbf{J}_c \odot \mathbf{t})(\mathbf{H}^N)^T = \hat{\mathbf{J}}_c^a \odot \hat{\mathbf{t}}_1 \tag{4.24}$$

Proof

Similarly, there exist:

$$\begin{aligned}
&\mathbf{H}^M(\mathbf{J}_c \odot \mathbf{t})(\mathbf{G}^N)^T(m,n) \\
&= \left(\frac{1}{4}\sum_{p,q\in\{0,1\}}(-1)^q \mathbf{J}_c(2m-p,2n-q)\right) \odot \mathbf{t}(2m,2n) \\
&= \hat{\mathbf{J}}_c^v \odot \hat{\mathbf{t}}_1(m,n)
\end{aligned} \tag{4.25}$$

$$\begin{aligned}
&\mathbf{G}^M(\mathbf{J}_c \odot \mathbf{t})(\mathbf{H}^N)^T(m,n) \\
&= \left(\frac{1}{4}\sum_{p,q\in\{0,1\}}(-1)^p \mathbf{J}_c(2m-p,2n-q)\right) \odot \mathbf{t}(2m,2n) \\
&= \hat{\mathbf{J}}_c^h \cdot \hat{\mathbf{t}}_1(m,n)
\end{aligned} \tag{4.26}$$

Proof

$$
\begin{aligned}
&\mathbf{G}^M(\mathbf{J}_c \odot \mathbf{t})(\mathbf{G}^N)^T(m,n) \\
&= \left(\frac{1}{4} \sum_{p,q \in \{0,1\}} (-1)^{(p+q)} \mathbf{J}_c(2m-p, 2n-q) \right) \odot \mathbf{t}(2m, 2n) \\
&= \hat{\mathbf{J}}_c^d \odot \hat{\mathbf{t}}_1(m,n) \qquad (4.27)
\end{aligned}
$$

Obviously, Equations (4.21), (4.24), (4.25), (4.26) and (4.27) constitute the Equation (4.17).

This completes the proof.

Model - Conclusion

This low dimension model can enable efficient dehazing processing by recovering $\hat{\mathbf{J}}_c^a$ and $\hat{\mathbf{t}^a}$, which are sufficient for further computing the solutions for $\hat{\mathbf{t}}$, $\hat{\mathbf{J}}_c$, t and $\mathbf{J}_c$ using the known $\hat{\mathbf{I}}_c$,$\mathbf{I}_c$ and the DHWT.

Optimisation

The proposed convex optimization for dehazing is based on the simplified DHWT model (3) with the known low sub band block $\hat{\mathbf{I}}_c^a$ and unknown $\hat{\mathbf{J}}_c^a$, $\hat{\mathbf{t}}^a$ and $\hat{\mathbf{a}}_c$.Because of the coupling term of $\hat{\mathbf{J}}_c^a \odot \hat{\mathbf{t}}^a$ with both $\hat{\mathbf{J}}_c^a$ and $\hat{\mathbf{t}}^a$ unknown,
the solution for $\hat{\mathbf{J}}_c^a$ and $\hat{\mathbf{t}}^a$ is a typical non-convex problem.
To formulate the convex optimization problem, introduce

$$\hat{\mathbf{Y}}_c^a = \hat{\mathbf{I}}_c^a - \hat{a}_c \hat{\mathrm{t}}^a, c = 1, 2, 3$$

and

$$\hat{\mathbf{Q}}_c^a = \hat{\mathbf{J}}_c^a \odot \hat{\mathbf{t}}^a$$

Then Equation(3) becomes

$$\hat{\mathbf{Y}}_c^a = \hat{\mathbf{Q}}_c^a - \hat{a}_c \hat{\mathrm{t}}^a, c = 1, 2, 3. \tag{4}$$

Optimisation

The reformulated model is linear in Q_c^a and t^a, which enables the following convex optimization.

$$\min_{\hat{\mathbf{Q}}_c^a, \hat{\mathbf{t}}^a} \quad \sum_{c=1,2,3} , (\|\hat{\mathbf{Y}}_c^a - \hat{\mathbf{Q}}_c^a + \hat{a}_c \hat{\mathrm{t}}^a\|_2^2) + R(\hat{\mathrm{t}}^a, \hat{\mathbf{Q}}_c^a, c = 1, 2, 3)$$

s.t. $0 \prec \hat{\mathbf{t}}^a \preceq 1, 0 \preceq \hat{\mathbf{Q}}_c^a, c = 1, 2, 3,$
where R($\hat{\mathrm{t}}^a, \hat{\mathbf{Q}}_c^a, c = 1, 2, 3$) denotes a convex regularization function of $\hat{\mathbf{Q}}_c^a$ and $\hat{\mathrm{t}}^a$ to be selected.

Optimisation

For selection of the regularization function, it is noted that the mean squared contrast of $\hat{\mathbf{J}}_c^a$ is given by

$$C_{ms} = \sum_{c=1,2,3;\ m,n\in\Omega_a} (\hat{J}_c^a(m,n) - \bar{J}_c^a)^2 / N_{\Omega_a}$$

$$= \sum_{c=1,2,3;\ m,n\in\Omega_a} \frac{(\hat{I}_c^a(m,n) - \bar{I}_c^a)^2}{(\hat{t}^a(m,n))^2 N_{\Omega_a}},$$

where Ω_a denotes the domain of the 2-dimensional pixel index, $\hat{J}_c^a$, $\hat{I}_c^a$ are the average pixel values of $\hat{J}_c^a$c and $\hat{I}_c^a$, respectively, and N_{Ω_a} is the total pixel number

Optimisation

$\Longrightarrow$ Improve the $C_{ms} value of the image$.
NOte that the difference between Q_a^c and $\hat{t}$ is the constant Y_a^c.
$\Longrightarrow$ to reduce the magnitude of Q_a^c , we can support the reduction of t^a.
$\Longrightarrow$ the smooth and low pass feature of $\hat{t}^a$ is to be promoted by regulating its total variation function.
Thus,the regularization function $Q_a^c, c = 1, 2, 3$ is specified as

$$R(\hat{\mathbf{t}}^a, \hat{\mathbf{Q}}_c^a, c = 1, 2, 3) = \lambda_1 \|\hat{\mathrm{t}}^a\|_2^2 + \lambda_2 \|\hat{\mathbf{t}}^a\|_{TV} + \lambda_3 \sum_{c=1,23} \|\hat{\mathbf{Q}}_c^a\|_2^2,$$

where $\|.\|_2$ and $\|.\|_{TV}$ denote the $\ell 2$ and total variation norms, respectively. It results in the following convex optimization.

Optimisation

$$\min_{\hat{\mathbf{Q}}_c^a, \hat{t}^a} \quad \sum_{c=1,23} (\|\hat{\mathbf{Y}}_c^a - \hat{\mathbf{Q}}_c^a + \hat{a}_c \hat{\mathrm{t}}^a\|_2^2) + \lambda_1 \|\hat{\mathbf{t}}^a\|_2^2 + \lambda_2 \|\hat{\mathbf{t}}^a\|_{TV} + \lambda_3 \sum_{c=1,23} \|\hat{\mathbf{Q}}_c^a\|_2^2, \tag{7}$$

$$\text{s.t.} \quad \mathbf{0} \prec \hat{\mathbf{t}}^a \preceq 1, \ \mathbf{0} \preceq \hat{\mathbf{Q}}_c^a, \ c = 1, 2, 3.$$

NOTE : Norm functions are convex in nature
Proof : Let f(x) = $\|x\|$
Applying Triangle Inequality,
$\|\theta x_1 + (1-\theta)x_2\| <= \theta\|x_1\| + (1-\theta)\|x_2\|$ Thus, from Jensen's Inequality, f is convex
This is the CO-DHWT algorithm.

Remarks

Remark 1: The idea and derivation for the proposed CO-DHWT is directly applicable to the original hazed image model (1), which can result in the following convex optimization for image dehazing, without the DHWT but with larger image dimension.

$$\begin{aligned} \min_{\mathbf{Q}_c,\mathbf{t}} \quad & \sum_{c=1,2,3} (\|\mathbf{Y}_c - \mathbf{Q}_c + a_c\mathbf{t}\|_2^2) \\ & + \lambda_1\|\mathbf{t}\|_2^2 + \lambda_2\|\mathbf{t}\|_{TV} + \lambda_3 \sum_{c=1,2,3} \|\mathbf{Q}_c\|_2^2, \\ \text{s.t.} \quad & \mathbf{0} \prec \mathbf{t} \preceq 1,\ \mathbf{0} \preceq \mathbf{Q}_c,\ c = 1,2,3, \end{aligned} \tag{8}$$

where Qc=Jc⊙t and Yc=Qc−ac1,c=1,2,3. This convex optimization without the DHWT is called CO in the rest of this paper.

Remarks

Remark 2: The idea and derivation for the proposed CO-DHWT is directly extendable to multilevel subband DHWT of the hazed image model. It can lead to transformed subband hazed image models with further reduced dimension and possible dehazing processing with further reduction of computational workload.

Computational Results

The proposed CO-DHWT (7) was implemented with the Split Bregman iteration algorithm [23] and coded with Matlab. The regularization parameters were empirically adjusted and set as $_1$=0.02,$_2$=0.002 and $_3$=0.04.